Journal of Molecular Liquids 310 (2020) 113196

Contents lists available at ScienceDirect

Journal of Molecular Liquids

journal homepage: www.elsevier.com/locate/molliq

Synthesis and photophysical insights of new fused N-heterocyclic derivatives with isoquinoline skeleton

Carmen Gherasim [a], Anton Airinei [a,*], Radu Tigoianu [a], Anda M. Craciun [a], Ramona Danac [b,*], Alina Nicolescu [a], Dragos Lucian Isac [a], Ionel I. Mangalagiu [b]

[a] Petru Poni Institute of Macromolecular Chemistry, Grigore Ghica Voda Alley 41A, Iasi 700487, Romania
[b] Alexandru Ioan Cuza University of Iasi, Chemistry Department, 11 Carol I Bd., Iasi 700506, Romania

ARTICLE INFO

Article history:
Received 12 March 2020
Received in revised form 14 April 2020
Accepted 19 April 2020
Available online 22 April 2020

Keywords:
Pyrrolo[2,1-*a*]isoquinoline
Imidazo[2,1-*a*]isoquinoline
Fluorescence
Quantum yields
Lifetimes

ABSTRACT

Six new fused isoquinoline based compounds (compounds **5a–c** with pyrrolo[2,1-*a*] isoquinoline structure and compounds **6a–c** with imidazo[2,1-*a*]isoquinoline skeleton) have been synthesized using the [3 + 2] cycloaddition of the several *in situ* generated cycloimmonium ylides to ethyl propiolate or ethyl cyanoformate. All the synthesized compounds have been investigated in solution by UV–VIS absorption, steady and time-resolved fluorescence methods. The effect of the substituents on the spectral characteristics has been demonstrated. These derivatives displayed an intense emission between 360 and 420 nm. The emission quantum yields ($\Phi = 0.54–0.64$) of pyrroloisoquinoline derivatives in dimethylsulfoxide (DMSO) were significantly higher than those of imidazoquinolines (0.03–0.16). The fluorescence decay of isoquinoline derivatives follows a biexponential law. A noticeable response of these isoquinoline derivatives to sodium hydroxide was observed.

1. Introduction

The application of polyheterocycles based on privileged structures as isoquinoline covers a vast therapeutic area [1–3]. For this reason, fused scaffolds containing isoquinoline have received much attention as drug candidates, a variety of improved synthetic methods being reported recently [4–8]. Among this class of compounds, pyrrolo[2,1-*a*]isoquinoline framework remarks as part of various synthesized compounds showing different biological activities, but also as part of many natural compounds as lamellarins, crispines, oleraceins and trollines [1]. Imidazo [2,1-*a*]isoquinoline is another skeleton of interest due to its biological properties including anti-inflammatory, anticancer, anti-HIV-1 or antimicrobial properties [9,10]. In addition to their biological properties, such molecules possess extended π-conjugated systems that make them excellent candidates for photophysical applications. Despite their huge potential in this field, there are only several reported studies regarding the fluorescence of molecules containing pyrrolo[2,1-*a*] isoquinoline or imidazo[2,1-*a*]isoquinoline core [11–15].

In that context and considering the growing interest for highly fluorescent materials with extended π-conjugation and their applications as sensors and biosensors, electroluminescent materials, lasers and other optoelectronic devices, we decided to synthesize several new pyrrolo [2,1-*a*]isoquinolines and imidazo[2,1-*a*]isoquinolines in order to realize a complete study regarding their photophysical properties and potential applications in the field.

2. Experimental

2.1. Materials and instrumentation

All reagents and solvents were commercially available and were used without further purification. For spectral measurements the solvents were of spectroscopic grade. ^{1}H NMR and ^{13}C NMR spectra were recorded on Bruker Avance III 500 MHz and Bruker Avance NEO 400 MHz spectrometers at room temperature. Coupling constants (*J*) are given in Hz. Chemical shifts were reported as relative values δ (ppm) to the residual signal of the deuterated solvent. The following abbreviations used to explain the multiplicity of the chemical shifts: s - singlet, d - doublet, t - triplet, q - quartet, m - multiplet, dd - doublet of doublet, as - apparent singlet. FTIR spectra were registered on a FT-IR Bruker Vertex 70 spectrophotometer (KBr discs). Thin layer chromatography (TLC) was performed using silica gel plates Merck 60 F_{254}. TLC plates were visualized using a UV lamp ($\lambda_{max} = 254$ or 365 nm). Melting points were determined on a Krüss Optronic melting point meter KSPI and are uncorrected. Electronic absorption spectra were measured

* Corresponding authors.
E-mail addresses: airineia@icmpp.ro (A. Airinei), rdanac@uaic.ro (R. Danac).

https://doi.org/10.1016/j.molliq.2020.113196
0167-7322/

with a SPECORD 200Plus Analytik Jena spectrophotometer using quartz cells with the light path length of 10 mm. The fluorescence spectra were obtained using a Perkin Elmer LS55 luminescence spectrometer in a 10 mm four-window quartz cuvette. The quantum yield of photoluminescence was determined on a FLS980 spectrometer using an integrating sphere. Dilute solutions (A < 1 at the excitation wavelength corresponding to the maximum of the first absorption band) were utilized for emission measurements. Luminescence decay curves were recorded on an Edinburgh FLS980 time-resolved single photon-counting fluorescence spectrometer using a 375 nm laser as excitation source. The time-resolved fluorescence decay curves were evaluated by fitting the spectral data to a sum of discrete exponentials: $I(t) = \Sigma a_i \exp(-t / \tau_i)$, where I(t) represents the fluorescence intensity at time t, τ_i and a_i are the emission decay time of component i and the pre-exponential factor, respectively, such that $\Sigma a_i = 1$. The fit quality has been estimated in terms of chi-squared (χ^2) and the visual analysis of the residuals.

2.2. Synthetic procedures

2.2.1. General procedure for synthesis of the quaternary isoquinolinium salts (**3a–c**)

All three monoquaternary isoquinolinium salts were prepared according to previously reported procedures [16,17]. Shortly, the starting substrate isoquinoline (**1**) (1 mmol, 1 eq.) was dissolved in acetone and then the corresponding halide (1 mmol, 1 eq.) was added. The reaction mixture was refluxed for 24 h under magnetic stirring. Subsequently, the reaction mixture was cooled at room temperature and the resulting precipitate was filtered and washed with acetone. The obtained monoquaternary salts (**3a–c**) have been used without purification in the next step.

2.2.2. General procedure for synthesis of the compounds **5a–c** and **6a–c**

The monoquaternary salts **(3a-c)** (1 mmol, 1 eq.) and dipolarophile (ethyl propiolate or ethyl cyanoformate) (1.1 mmol, 1.1 eq.) were suspended in chloroform (10 mL). Then triethylamine (3 mmol, 3 eq.) was added dropwise under magnetic stirring and nitrogen atmosphere. The obtained reaction mixture was refluxed with vigorous stirring for 24 h under nitrogen. After cooling at room temperature, to the resulting solution, 5 mL of methanol was added, and the mixture was kept without stirring until a precipitate was obtained. The solid was filtered and washed with a small amount of methanol to give the desired compound.

Ethyl 3-cyanopyrrolo[2,1-a]isoquinoline-1-carboxylate (**5a**). Orange solid, η = 63%, m.p. = 137–139 °C. IR (KBr, cm^{-1}): 3120, 2973, 2224, 2848, 1716, 1684, 1501, 1365, 1199. ^{1}H NMR ($CDCl_3$, 500 MHz): δ = 1.43 (t, *J* = 7.0 Hz, 3H, $CH_2\underline{CH_3}$), 4.39 (q, *J* = 7.0 Hz, 2H, $\underline{CH_2}CH_3$), 7.13 (d, *J* = 7.00 Hz, 1H, H_5), 7.57–7.66 (3H, overlapped signals, H_7, H_8, H_6), 7.77 (s, 1H, H_2), 7.98 (d, *J* = 7.0 Hz, 1H, H_4), 8.85 (d, *J* = 8.5 Hz, 1H, H_9). ^{13}C NMR ($CDCl_3$, 125 MHz): δ = 14.5 $CH_2\underline{CH_3}$, 60.9 $\underline{CH_2}CH_3$, 98.3 C_3, 110.5 C_1, 112.5 C_{14}, 116.0 C_5, 122.2 C_4, 124.9 C_{11}, 126.1 C_2, 127.2 C_6, 127.8 C_9, 128.5 C_8, 129.6 C_{10}, 129.4 C_7, 134.9 C_{12}, 163.7 C_{13}. Anal. calc. for $C_{16}H_{12}N_2O_2$: C 72.72; H 4.58; N 10.60. Found: C 72.76; H 4.50; N 10.64.

1-Ethyl 3-methyl pyrrolo[2,1-a]isoquinoline-1,3-dicarboxylate (**5b**). White solid, η = 80%, m.p. = 138–140 °C. IR (KBr, cm^{-1}): 3132, 2975, 2951, 1693, 1457, 1376, 1228, 1187, 1082, 762. ^{1}H NMR ($CDCl_3$, 500 MHz): δ = 1.45 (t, *J* = 7.0 Hz, 3H, $CH_2\underline{CH_3}$), 3.94 (s, 3H, OCH_3), 4.42 (q, *J* = 7.0 Hz, 2H, $\underline{CH_2}CH_3$), 7.18 (d, *J* = 7.5 Hz, 1H, H_5), 7.59–7.65 (2H, overlapped signals, H_7, H_8), 7.71 (d, *J* = 8.0 Hz, 1H, H_6), 8.04 (s, 1H, H_2), 9.37 (d, *J* = 7.5 Hz, 1H, H_4), 9.82 (d, *J* = 8.5 Hz, 1H, H_9). ^{13}C NMR ($CDCl_3$, 125 MHz): δ = 14.6 $CH_2\underline{CH_3}$, 51.7 OCH_3, 60.7 $\underline{CH_2}CH_3$, 109.9 C_1, 115.1 C_5, 115.7 C_3, 124.4 C_4, 125.1 C_{11}, 125.5 C_2, 126.8 C_6, 127.8 C_9, 127.9 C_8, 129.0 C_7, 129.8 C_{10}, 136.1 C_{12}, 161.6 C_{14}, 164.9 C_{13}. Anal. calc. for $C_{17}H_{15}NO_4$: C, 68.68; H, 5.09; N, 4.71%. Found: C, 68.65; H, 5.01; N, 4.73%.

Diethyl pyrrolo[2,1-a]isoquinoline-1,3-dicarboxylate (**5c**). White solid, η = 64%, m.p. = 126–129 °C. IR (KBr, cm^{-1}): 3128, 2980, 1709, 1697, 1376, 1232, 1077, 787. ^{1}H NMR ($CDCl_3$, 500 MHz): δ = 1.42–1.47 (6H, overlapped signals, 2 × $CH_2\underline{CH_3}$), 4.39–4.45 (4H, overlapped signals, 2 × $\underline{CH_2}CH_3$), 7.19 (d, *J* = 7.5 Hz, 1H, H_5), 7.60–7.66 (2H, overlapped signals, H_7, H_8), 7.72 (d, *J* = 8.0 Hz, 1H, H_6), 8.05 (s, 1H, H_2), 9.40 (d, *J* = 7.0 Hz, 1H, H_4), 9.82 (d, *J* = 8.0 Hz, 1H, H_9). ^{13}C NMR ($CDCl_3$, 125 MHz): δ = 14.7 2 × $CH_2\underline{CH_3}$, 60.7 2 × $\underline{CH_2}CH_3$, 109.8 C_1, 115.1 C_5, 116.1 C_3, 124.5 C_4, 125.1 C_{11}, 125.3 C_2, 127.2 C_6, 127.8 C_9, 127.9 C_8, 129.0 C_7, 129.8 C_{10}, 136.1 C_{12}, 161.2 C_{14}, 165.0 C_{13}. Anal. calc. for $C_{18}H_{17}NO_4$: C 69.44; H 5.50; N 4.50. Found: C 69.48; H 5.42; N 4.54.

Ethyl 3-cyanoimidazo[2,1-a]isoquinoline-2-carboxylate (**6a**). White solid, η = 40%, m.p. = 207–209 °C. IR (KBr, cm^{-1}): 2929, 2224, 1708, 1536, 1374, 1257, 1156, 793. ^{1}H NMR ($CDCl_3$, 500 MHz): δ = 1.51 (t, *J* = 7.0 Hz, 3H, $CH_2\underline{CH_3}$), 4.57 (q, *J* = 7.0 Hz, 2H, $\underline{CH_2}CH_3$), 7.44 (d, *J* = 7.50 Hz, 1H, H_5), 7.77 (2H, overlapped signals, H_7, H_8), 7.85 (dd, *J* = 6.5; 3.0 Hz, 1H, H_6), 8.15 (d, *J* = 7.0 Hz, 1H, H_4), 8.85 (dd, *J* = 8.5; 3.5 Hz, 1H, H_9). ^{13}C NMR ($CDCl_3$, 125 MHz): δ = 14.4 CH_2CH_3, 62.5 CH_2CH_3, 103.0 C_3, 110.3 C_{14}, 117.6 C_5, 121.3 C_4, 122.3 C_2, 123.4 C_{11}, 125.0 C_9, 127.6 C_6, 129.8 C_8, 130.7 C_{10}, 130.9 C_7, 145.2 C_{12}, 160.9 C_{13}. Anal. calc. for $C_{15}H_{11}N_3O_2$: C 67.92; H 4.18; N 15.84. Found: C 67.96; H 4.10; N 15.91.

2-Ethyl 3-methyl imidazo[2,1-a]isoquinoline-2,3-dicarboxylate (**6b**). White solid, η = 40%, m.p. = 142–146 °C. IR (KBr, cm^{-1}): 3125, 2992, 1739, 1716, 1392, 1214, 806. ^{1}H NMR ($CDCl_3$, 500 MHz): δ = 1.45 (t, *J* = 7.0 Hz, 3H, $CH_2\underline{CH_3}$), 3.98 (s, 3H, OCH_3), 4.51 (q, *J* = 7.0 Hz, 2H, $\underline{CH_2}CH_3$), 7.30 (d, *J* = 7.5 Hz, 1H, H_5), 7.66–7.70 (2H, overlapped signals, H_7, H_8), 7.77 (dd, *J* = 6.0; 3.0 Hz, 1H, H_6), 8.75 (dd, *J* = 6.0; 3.5 Hz, 1H, H_9), 8.93 (d, *J* = 7.5 Hz, 1H, H_4). ^{13}C NMR ($CDCl_3$, 125 MHz): δ = 14.4 $CH_2\underline{CH_3}$, 52.3 OCH_3, 62.1 $\underline{CH_2}CH_3$, 115.9 C_5, 116.4 C_3, 123.1 C_{11}, 123.5 C_4, 124.7 C_9, 127.0 C_6, 128.8 C_8, 130.1 C_7, 130.5 C_2, 141.5 C_{10}, 144.8 C_{12}, 160.5 COO, 164.0 COO. Anal. calc. for $C_{16}H_{14}N_2O_4$: C 64.42; H 4.73; N 9.39. Found: C 64.46; H 4.69; N 9.45.

Diethyl imidazo[2,1-a]isoquinoline-2,3-dicarboxylate (**6c**). Cream solid, η = 35%, m.p. = 133–135 °C. IR (KBr, cm^{-1}): 3138, 2988, 1732, 1706, 1403, 1216, 807. ^{1}H NMR ($CDCl_3$, 500 MHz): δ = 1.43 (t, *J* = 7.0 Hz, 3H, $CH_2\underline{CH_3}$), 1.46 (t, *J* = 7.0 Hz, 3H, $\underline{CH_2}CH_3$), 4.46 (q, *J* = 7.0 Hz, 2H, $CH_2\underline{CH_3}$), 4.51 (q, *J* = 7.0 Hz, 2H, $\underline{CH_2}CH_3$), 7.33 (d, *J* = 7.5 Hz, 1H, H_5), 7.70–7.73 (2H, overlapped signals, H_7, H_8), 7.80 (dd, *J* = 6.0; 3.5 Hz, 1H, H_6), 8.82 (dd, *J* = 6.0; 3.5 Hz, 1H, H_9), 9.67 (d, *J* = 7.5 Hz, 1H, H_4). ^{13}C NMR ($CDCl_3$, 125 MHz): δ = 14.3 $CH_2\underline{CH_3}$, 14.4 $CH_2\underline{CH_3}$, 62.0 $\underline{CH_2}CH_3$, 62.3 $\underline{CH_2}CH_3$, 116.0 C_5, 116.5 C_3, 123.0 C_{11}, 123.6 C_4, 124.9 C_9, 127.1 C_6, 128.9 C_8, 130.3 C_7, 130.6 C_2, 141.2 C_{10}, 144.6 C_{12}, 160.1 COO, 164.0 COO. Anal. calc. for $C_{17}H_{16}N_2O_4$: C 65.38; H 5.16; N 8.79. Found: C 65.36; H 5.09; N 8.87.

3. Results and discussion

The chosen method for the assembly of fused target polyheterocycles relied on 1,3-dipolar cycloaddition [8,16] of different isoquinolinium ylides to ethyl propiolate or ethyl cyanoformate. First, isoquinoline **1** (Scheme 1) was used together with halides **2a–c** for the synthesis of the monoquaternary salts **3a–c** [17,18]. As shown in Scheme 1, ethyl propiolate was reacted first with the corresponding isoquinolinium ylides **4a–c** (*in situ* generated in basic medium from salts **3a–c**) to give the intermediate dihydropyrrolo[2,1-*a*]isoquinolines **5′a–c**, which in turn underwent oxidative dehydrogenation under atmospheric conditions, yielding the final compounds **5a–c** in good yields (63–80%). Compound **5c** was obtained also by Chen using a different recently reported approach [19]. Using ethyl cyanoformate as dipolarophile in similar conditions, we obtained imidazo[2,1-*a*] isoquinolines **6a–c** presumably *via* dihydroderivatives **6′a–c**. All compounds have been fully characterized using spectral methods (IR, NMR) and quantitative elemental analyses (C, H, N). The NMR spectra prove the formation of the new fully aromatized pyrrolo[2,1-*a*]

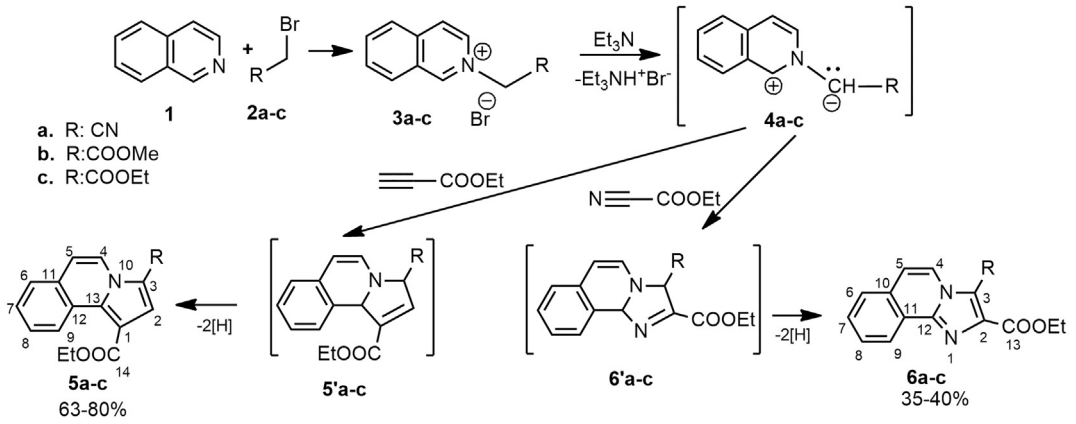

Scheme 1. Synthetic pathway for pyrrolo[2,1-*a*]isoquinolines **5a–c** and imidazo[2,1-*a*]isoquinolines **6a–c**.

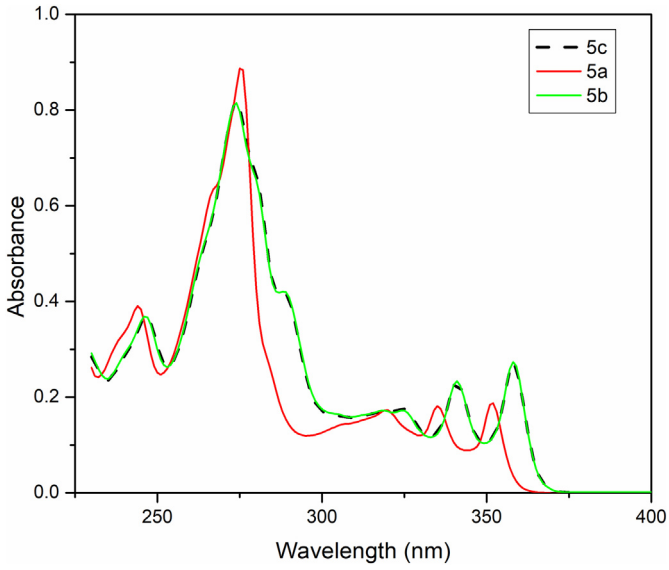

Fig. 1. UV–Vis absorption spectra of pyrroloisoquinolines **5a–c** in dichloromethane.

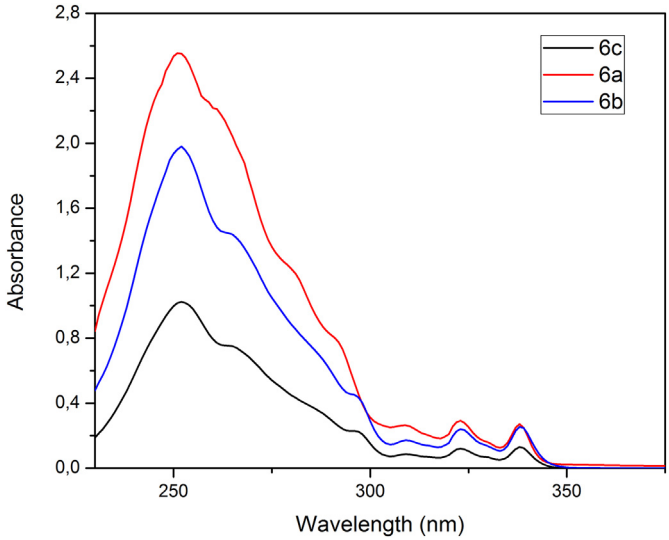

Fig. 2. Electronic absorption spectra of imidazoisoquinolines **6a–c** in dichloromethane.

isoquinoline cycle in case of compounds **5a–c** and imidazo[2,1-*a*] isoquinoline cycle in case of compounds **6a–c**.

The electronic absorption spectra of pyrroloisoquinolines **5a–c** display three main absorption bands located in the following ranges in dichloromethane (DCM): 300–400 nm, 260–300 nm and around 240 nm, respectively (Fig. 1). The absorption band at longer wavelengths presents a vibronic structure with an absorption maximum at 340 nm for **5b**, **5c** and at 356 nm for **5a**. This absorption band can be assigned to a π-π* transition of the pyrroloisoquinoline ring [12]. The substituents on the nitrogen ring can exert a significant effect on the position of absorption and emission bands of these isoquinoline derivatives. The absorption spectra of compounds **5b** and **5c** are practically similar (Fig. 1), while the introduction of CN group in the position 3 on the pyrrole ring induces a prominent hypsochromic shift of the longer wavelength absorption band of **5a** (Fig. 1). It can be seen in Fig. 2 that the absorption spectra of imidazoisoquinolines **6a–c** differ from the ones of the pyrrolo derivatives **5a–c**. Thus, the imidazoisoquinolines **6a–c** exhibit two main absorption bands: a lower intensity long wavelength band with vibrational structure (300–350 nm), centered at about 323 nm as well as two absorption bands at 339 and 309 nm, on both sides of the central absorption maximum and a high intensity broad absorption band with an absorption maximum around 250 nm in dichloromethane (Fig. 2).

The red-shift absorption profile observed when compared to imidazoisoquinolines can be attributed to the extended π-π* conjugation in this system due to the substituents from the positions 1 and 3 on the pyrrole ring. The blue shift of the absorption band from longer wavelengths in pyrroloisoquinolines occurs also in DMSO (Table 1). The spectral pattern of pyrroloisoquinolines **5b** and **5c** is much less influenced by the presence of substituents in the positions 1 and 3 on the pyrrole ring (COOMe, COOEt). As shown in Table 1, the electronic absorption spectra of pyrrolo- and imidazo- isoquinolines showed

Table 1
Photophysical properties of isoquinoline derivatives.

Sample	Solvent	λ_{max} (nm)	λ_{em} (nm)	Φ (%)
5a	DCM	352, 335, 320, 275, 244	356, 374, 392, 415sh	28.37
	DMSO	353, 336, 321, 276	359, 376, 395, 415sh	63.47
5b	DCM	358, 341, 325, 274, 246	363, 381, 401, 425sh	20.10
	DMSO	358, 341, 325, 275	361, 382, 401, 425sh	53.95
5c	DCM	358, 341, 324, 274, 247	363, 381, 401, 425sh	31.28
	DMSO	358, 341, 325sh, 275	364, 382, 400, 425sh	55.76
6a	DCM	338, 323, 309, 252	340, 356, 375, 395sh	41.04
	DMSO	339, 324, 309	345, 361, 378	3.36
6b	DCM	338, 323, 309, 251	344, 360, 374, 400sh	18.37
	DMSO	339, 324, 309	346, 360, 374	7.96
6c	DCM	338, 323, 309, 252	344.5, 359, 375, 400sh	29.41
	DMSO	339, 323, 309	346, 359, 372	15.95

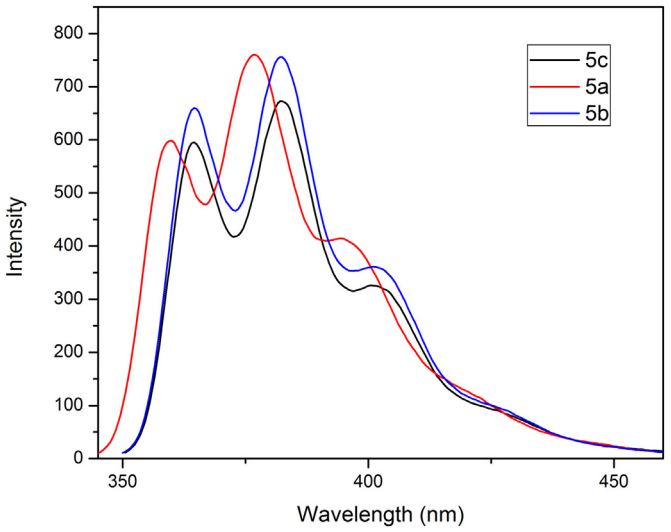

Fig. 3. Fluorescence spectra of isoquinoline derivatives **5a–c** in DMSO (λ_{ex} = 275 nm).

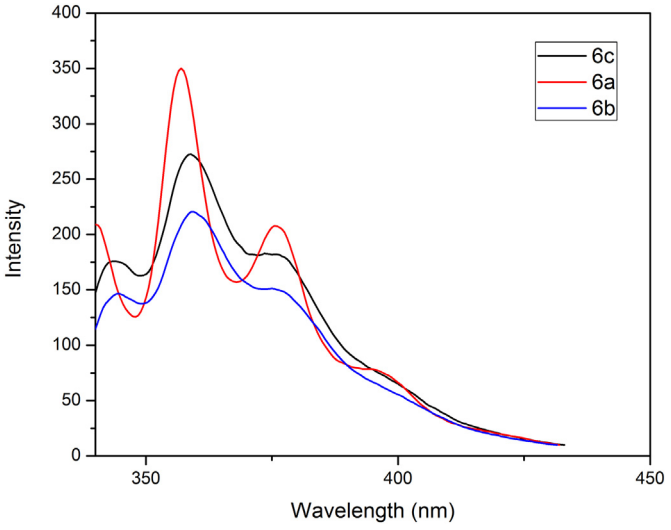

Fig. 4. Emission spectra of isoquinoline derivatives **6a–c** in dichloromethane (λ_{ex} = 339 nm).

almost no changes in solvent with different polarities, suggesting that the ground state of these derivatives is not significantly modified by solvent polarity.

The emission spectra of derivatives **5a–c** in DMSO at room temperature when excited at their absorption maxima are depicted in Fig. 3. The emission bands for **5b** and **5c** are located at 363, 381 and 401 nm, respectively, with a shoulder band around 425 nm. Similar to absorption spectra, the emission maxima of **5a** containing CN group on the pyrrole ring are shifted to shorter wavelengths both in DCM and DMSO (Fig. 3, Table 1). Also, the position of the emission maxima was not affected by the increase of solvent polarity (Table 1). The fluorescence bands of imidazoisoquinolines **6a-c** were found in the spectral range 350–420 nm (Fig. 4). The position of emission bands for derivatives **6a–c** is not practically influenced by the substituents on the pyrrole ring excepting compound **6a** which displays a blue shift in dichloromethane (Fig. 4, Table 1). Compared to pyrroloisoquinoline derivatives **5a–c**, the emission bands of imidazoisoquinolines **6a–c** are blue shifted in DCM and DMSO. The values of absorption and emission maxima as well as the values of fluorescence quantum yields and fluorescence lifetimes of the isoquinolines derivatives are collected in Table 1.

The emission quantum yield values of isoquinoline derivatives are strongly dependent on the substituent and the solvent nature. The fluorescence quantum yield had the highest values in DMSO for pyrroloisoquinolines **5a–c** (Φ = 63.47% for **5a**) (Table 1). However, the fluorescence quantum yield of derivatives **5a–c** is significantly reduced in dichloromethane (*e.g.* in case of compound **5b**, the quantum yield decreased from 53.95% in DMSO to 20.10% in DCM). The quantum efficiencies (Φ) of imidazoisoquinolines **6a–c** ranged from 18.37% to 41.04% in DCM and from 3.36% to 15.95% in DMSO, respectively (Table 1). Thus, the pyrroloisoquinolines show much higher emission quantum yields in DMSO than imidazoisoquinolines, while in DCM close values of quantum efficiencies were found for **5b–c** and **6b-c** derivatives. The exception is product **6a** which provided a high quantum yield in DCM of 41.04% by comparison with **5a** (Φ = 28.37%). These results revealed that the presence of CN acceptor groups determines an important enhancement of quantum yield in DMSO for pyrroloisoquinolines **6a** (63.47%) and in DCM for imidazoisoquinolines **6a** (41.04%). The substituent –COOMe in the position 3 on the pyrrole and imidazo rings affected the emission as the compounds **5b** and **6b** displayed the lowest values of quantum yield in DCM (20.10% and 18.37%, respectively). It is worth noting that COOEt substituent on the imidazole ring induced an increase of quantum yield for **6c** in DMSO (Table 1). The quantum yield values of derivatives **6a–c** are higher in DCM because the non-radiative processes in these compounds are diminished in solvents having low polarity [20].

The luminescence lifetimes has been determined by time-correlated single photon counting (TCSPC) technique. Emission decays for all investigated compounds were found to be the best characterized by a double-exponential function in DMSO over the entire emission range.

The radiative rate constant, k_r, and the non-radiative rate constant k_{nr}, for isoquinolines derivatives can be estimated from the determined emission quantum yield (Φ) and the double-exponential emission decay lifetimes (τ) using the following relations:

$$k_r = \frac{\Phi}{\tau}$$

and

$$k_{nr} = \frac{1-\Phi}{\tau}$$

Table 2
Decay parameters of isoquinoline derivatives in DMSO.

Sample	τ_1 (ns)	τ_2 (ns)	a_1%	a_2%	χ	$k_r^1 * 10^{-9}$ (ns)	$k_{nr}^1 * 10^{-9}$ (ns)	$k_r^2 * 10^{-9}$ (ns)	$k_{nr}^2 * 10^{-9}$ (ns)
5a	0.069	3.115	94.42	5.58	0.99	9.19	5.29	0.20	0.12
5b	0.866	3.095	27.17	72.83	0.99	0.64	0.51	0.18	0.14
5c	0.112	3.219	4.59	95.41	0.99	4.82	4.11	0.17	0.14
6a	0.031	2.785	89.46	10.54	0.99	1.10	31.68	0.01	0.35
6b	0.060	2.700	98.30	1.70	1.00	1.33	15.34	0.03	0.34
6c	0.036	5.400	99.63	0.37	0.99	4.43	23.35	0.03	0.16

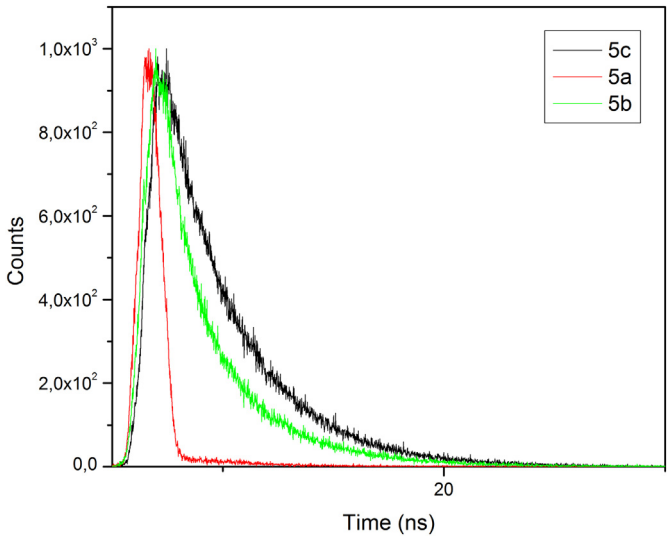

Fig. 5. Time-resolved decay profile of **5a–c** in DMSO.

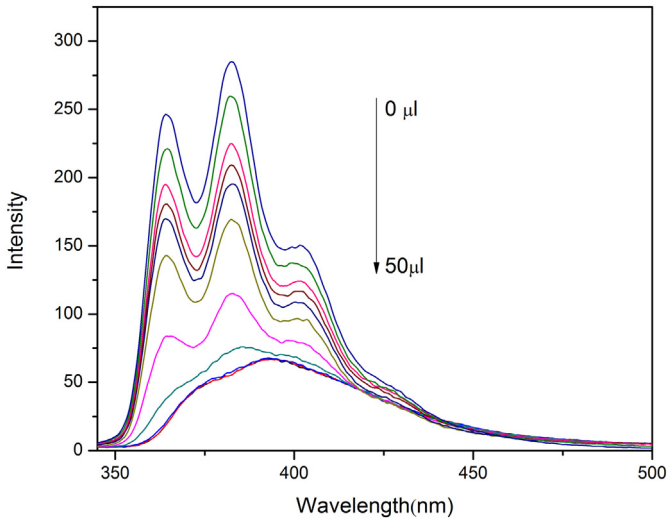

Fig. 7. Effect of NaOH addition on the emission spectra of **5c** (λ_{ex} = 275 nm).

The values of the fluorescence lifetimes (τ_j) and rate constants (k_r, k_{nr}), as well as their intensity amplitudes (a_i) are summarized in Table 2.

Representative time-resolved profiles of pyrroloisoquinolines **5a–c** and imidazoisoquinolines **6a–c** in DMSO are depicted in Figs. 5 and 6. The decay patterns were fitted to the double exponential model, indicating probably the formation of two geometrical conformers for all derivatives. We would like to mention that the lifetime τ_1 is always shorter than τ_2 at a particular emission wavelength (Table 2). The fluorescence lifetime τ_1 of pyrroloisoquinolines **5a–c** were longer than those of imidazoisoquinolines **6a–c** (Table 2) in DMSO. For derivatives **5a–c** the short-lived component of lifetime varies in the range of 0.069 to 0.866 ns, the shortest values of τ_1 being observed for **5a** (Table 2). However, the contributions corresponding to the τ_2 long-lived component increase for **5b** and **5c**, being 72.83 and 95.41%, respectively, whereas for **5a** the contribution from τ_1 becomes predominant (94.42%). In the case of imidazoisoquinolines the lifetime values of τ_2 are higher than τ_1 and the major contribution results from the short-lived components of τ_1 with amplitudes of 98.3, 99.6 and 89.5%, respectively. An extension of the long-lived component of lifetime was observed for **6a**. The values of the rate constant of radiative deactivation (k_r) estimated from the lifetimes of the short-lived component of the fluorescence decay increased from $0.64 * 10^9$ to $9.19 * 10^9$ s^{-1} in the series of pyrroloisoquinolines, the greatest value being attained for compound **5a**. Following the changes in the quantum yield values and lifetimes, the same tendency was also observed for non-radiative rate constants (k_{nr}) of the both classes of isoquinolines. The values of k_r determined for these isoquinolines derivatives are higher when compared to those estimated for other quinoline compounds [21,22].

To study the changes of the absorption and fluorescence spectra in the presence of NaOH 0.1 N, titration experiments with various amounts of NaOH were performed. The addition of NaOH 0.1 N determines the progressive decrease of the emission intensity of **5c**, without the modification of emission profile in the first stages of NaOH addition (Fig. 7). The change in the emission spectra of **5c** during the addition of NaOH occurs at 30 μl of NaOH, when the emission band becomes broad and structureless with a maximum located at 390 nm. Adding higher amounts of NaOH does not change the emission profile (Fig. S1). Also, in case of compound **5b**, the intensity of the long wavelength absorption band decreases up to 40 μl by adding NaOH and then the vibrational subbands become broader with a small decrease in intensity and a shift to longer wavelengths (Fig. 8).

The recovery of the emission band centered at 382 nm for **5c** was noticed by adding HCl 0.1 N to the solution containing NaOH (Fig. S2) and the initial emission spectrum was restored. We would like to mention

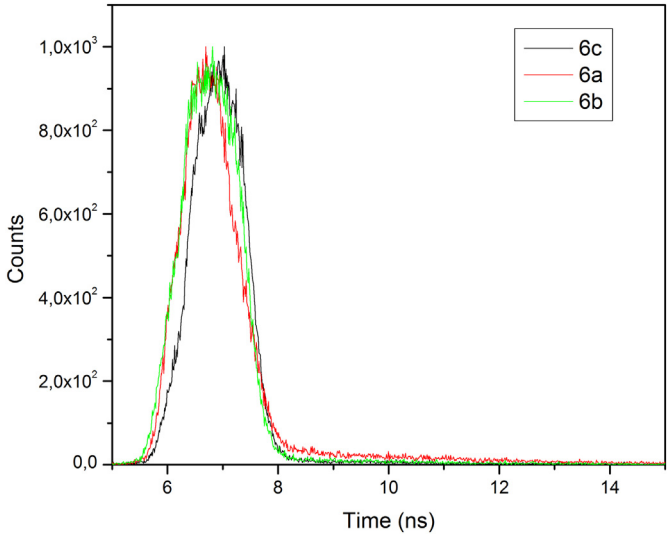

Fig. 6. Profiles of emission decay of **6a–c** in DMSO.

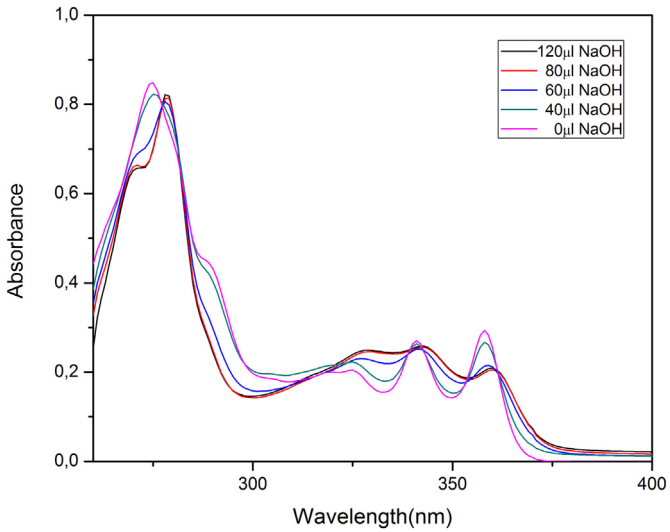

Fig. 8. Evolution of the absorption spectra of **5b** upon addition of NaOH.

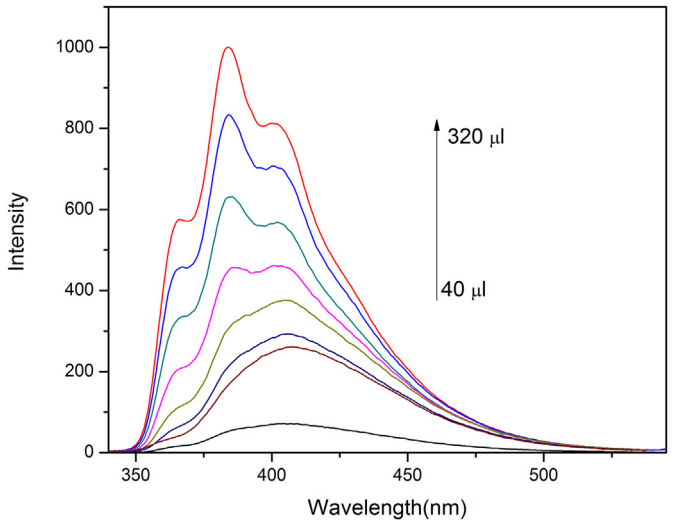

Fig. 9. Evolution of the emission spectra of **5a** upon addition of different NaOH levels ($\lambda_{ex} = 278$ nm).

that the absorption or emission spectra after 24 h have the same profile confirming the stability of derivative **5c** in basic medium.

The other pyrroloisoquinoline derivatives (**5a**, **5b**) exhibited similar modifications in the emission and absorption spectra by adding NaOH in the first stages (Figs. S3–S5). However, these changes occurred faster for **5a** after adding only 20 μl of NaOH and the broad emission band was located at 390 nm. At higher addition levels of NaOH (>40 μl), the emission band of **5a** at about 410 nm increases gradually in intensity and the initial profile of the emission band was restored (Fig. 9).

The sensitivity of pyrroloisoquinoline derivatives in the presence of NaOH has been checked by NMR titration experiments in DMSO-d_6. Results are presented in Fig. 10 for derivative **5a**. The NMR data indicated that a hydrolysis reaction took place on both ester and cyano groups, with formation of a sodium dicarboxylate derivative. The ^{1}H NMR spectra recorded during the NaOH titration experiment contained several sets of signals, with variable intensities, suggesting the presence of more derivatives. As can be seen in Fig. 10 four spectra recorded after the addition of different volumes of NaOH are presented for derivative **5a**, illustrating the formation and the disappearance of two intermediary derivatives. For a better visualization, only the region 7–8 ppm is given, the signals of interest being the two doublets from 7.22 and 7.31 ppm, respectively, assigned to the proton in position 5 in the two intermediary derivatives. Valuable information about the structure of these intermediary derivatives was obtained from a long-range proton-carbon correlation experiment (H,C-HMBC) illustrated in Fig. 11. For one derivative, correlations were obtained between the proton in position 2 (a singlet at 8.00 ppm) and ester carboxylic carbon from 164.6 ppm, indicating a derivative with unaffected ester group and hydrolyzed cyano group (the follow-up signal is the doublet from 7.31 ppm, Fig. 10). Other correlation supporting this conclusion was made between the ester carboxylic carbon from 164.6 ppm and methylene protons (quartet centered at 4.32 ppm) Figs. 11, S6). For the other intermediary derivatives, there was no correlation with ester carboxylic

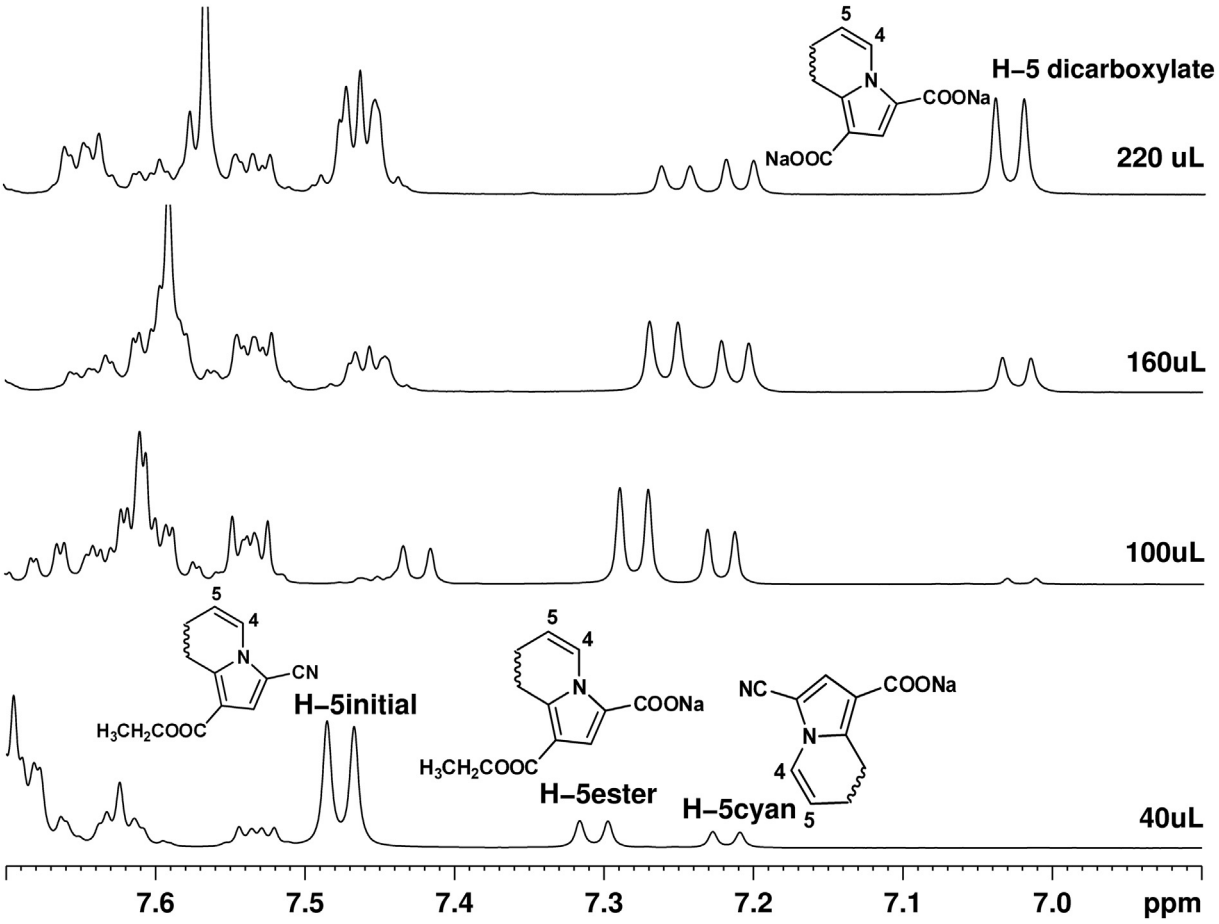

Fig. 10. Evolution of ^{1}H NMR spectra for **5a** after addition of different volumes of NaOH, illustrating the hydrolysis of ester and cyano groups, with the formation of two intermediary derivatives.

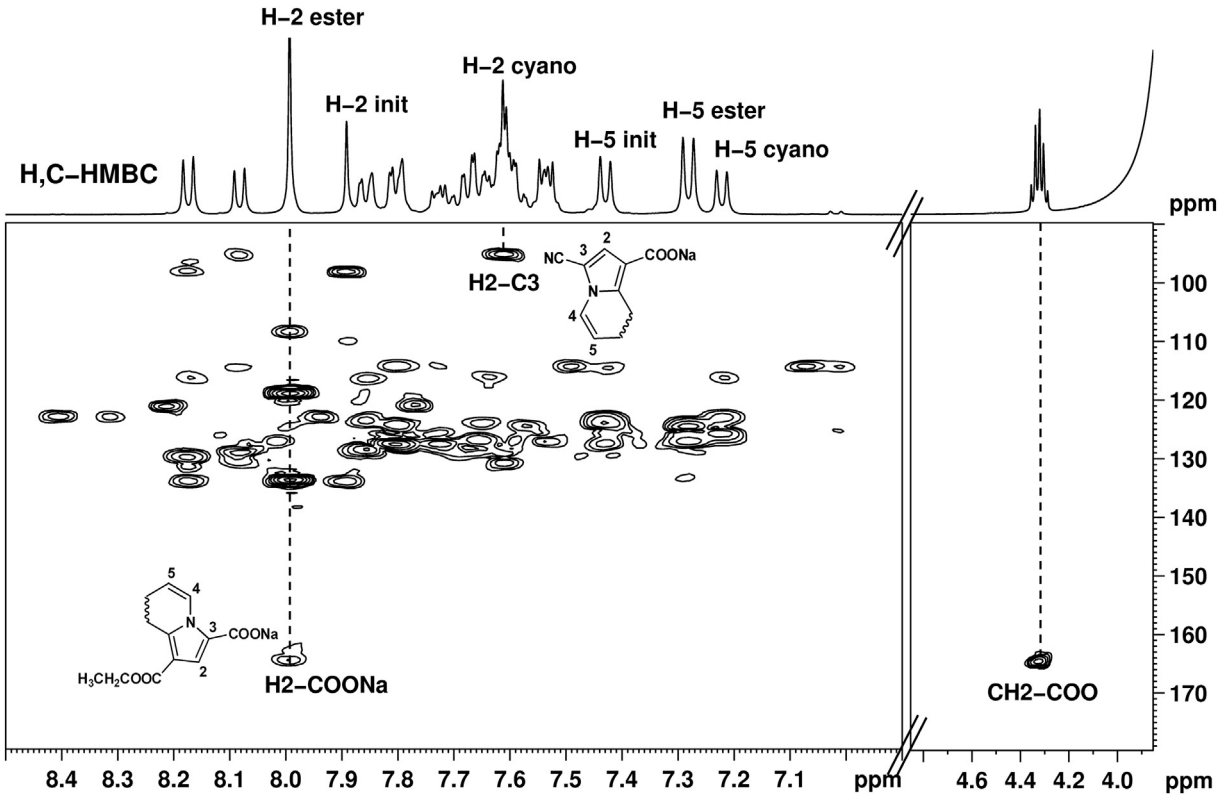

Fig. 11. H,C-HMBC spectrum for **5a** after the addition of 90 μl NaOH 0.1 N. The correlations of interest proving the existence of the two intermediary compounds are marked in the 2D plot.

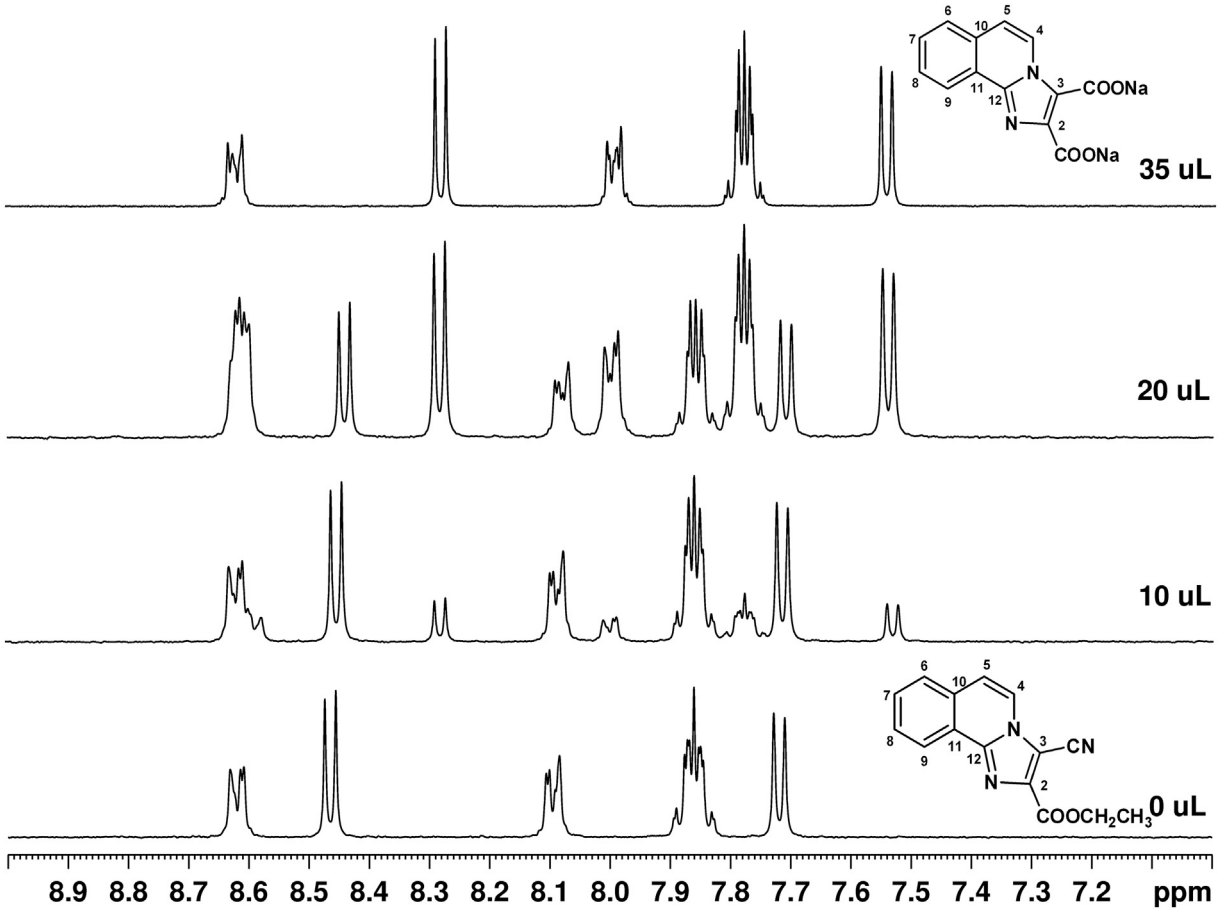

Fig. 12. Change in the ^{1}H NMR spectrum of **6a** upon addition of different volumes of NaOH, illustrating the hydrolysis of ester and cyano groups, with the formation of the sodium dicarboxylate derivative.

carbon. Instead, a correlation between the proton in position 2 (a singlet at 7.61 ppm) and a quaternary carbon from 95.3 ppm, assigned to carbon in position 3, when it is chemically bonded with cyano group was observed. This fact suggested an intermediary derivative with an unaffected cyano group and hydrolyzed ester group (the follow-up signal is the doublet from 7.22 ppm, Fig. 10).

The titration experiment was stopped when only one set of signals was observed in the ^{1}H NMR spectrum, suggesting the presence of a single final derivative. Long-range correlation signals between the proton in position 2 and the two quaternary carbons from 165.3 and 172.1 ppm, indicated the presence of two carboxylic groups in the structure of the final compound (the follow-up signal is the doublet from 7.02 ppm, Fig. 10). Because the number and the shape of the signals at the end of the titration experiment were similar with that of the initial compound, we concluded that the rest of the structure remained intact, the hydrolysis of the ester and cyano groups being the only chemical modifications. The formation of the ethanol during NaOH titration was followed in the ^{1}H NMR spectra through the characteristic signals from 1.03 ppm (triplet, assigned to methyl protons) and 3.45 ppm (quartet, assigned to methylene protons). A similar titration experiment was performed for compound **5b**. In this case, the hydrolysis of the ester and cyano groups occurs, with the formation of corresponding sodium carboxylate derivative and ethanol (Fig. S7). During NaOH titration, the vibronic structure of the absorption band at longer wavelengths is diminished, the absorption bands become broader and their intensities do not change (Fig. S5), probably due to the presence of more species close structurally in system according to NMR data.

Adding different amounts of NaOH 0.1 N to a DMSO solution of imidazoisoquinoline **6c**, its emission intensity decreases progressively and after additions of 70 μl NaOH a new broad emission band appeared at about 400 nm. This emission band increases in intensity adding new NaOH aliquots (Fig. 12). As anticipated, the addition of hydrochloric acid to the basic solution of **6c** determines the increase of emission intensity to the starting value (Fig. S9). The spectral emission behaviour of derivatives **6a** and **6b** was similar to that observed for related compounds **5c** and **5b**, respectively (Figs. S10, S11). Also, the titration experiment made for compound **6a** takes place with the hydrolysis of the ester and cyano groups and the appearance of the corresponding sodium carboxylate derivative and ethanol (Fig. 13).

The effect of hydrochloric acid on the emission and absorption bands of isoquinoline derivatives was investigated in DMSO solutions. The addition of HCl 0.1 N leads to a small decrease of the intensity in the fluorescence spectra range between 10 and 15% for imidazo- and pyrroloisoquinoline derivatives (Fig. S12). The addition of higher amounts of HCl did not change the emission spectral pattern. In acidic medium the absorption spectra of these derivatives are practically similar. As reported in literature, for other pyrrazoloisoquinoline derivatives the presence of an acid modifies significantly the absorption and emission spectra due to the protonation effect of the acid [14,23].

The fluorescence signal of **6c** was investigated in organic solvents containing various amount of water. The study was made in DMSO as polar aprotic solvent. The influence of water content on the emission spectra of **6c** was depicted in Fig. 14. As can be seen from Fig. 14 the emission intensity of **6c** gradually decreased with increasing water content. Upon incremental addition of water into the solution, the emission band shifts to longer wavelengths and a new broad and structureless emission band centered at 410 nm appeared (Fig. 14). At the same time, the intensity of longer wavelength absorption band decreased in intensity as the water content increased without other change in the absorption spectra.

4. Conclusions

A series of luminescent fused N-heterocyclic derivatives with isoquinoline skeleton was successfully synthesized and characterized. The pyrroloisoquinoline derivatives exhibited strong fluorescence with maxima ranged between 350 and 420 nm and high quantum yields in DMSO solution, values much higher that imidazoisoquinoline compounds. All compounds exhibited excited-state lifetimes in the nanosecond timescale. Emission bands of pyrroloisoquinoline derivatives **5a-c** occur at wavelengths over 350 nm and they are clear hypsochromic shifts of the absorption and emission bands provided by imidazoisoquinolines **6a-c**. ^{1}H NMR titration experiments with NaOH revealed that the hydrolysis occurred to cyano and ester groups with the formation of a sodium dicarboxylate derivative.

Authorship statement

All persons who meet authorship criteria are listed as authors, and all authors certify that they have participated sufficiently in the work to take public responsibility for the content, including participation in the concept, design, analysis, writing, or revision of the manuscript. Furthermore, each author certifies that this material or similar material has not been and will not be submitted to or published in any other publication before its appearance in the *Journal of Molecular Liquids.*

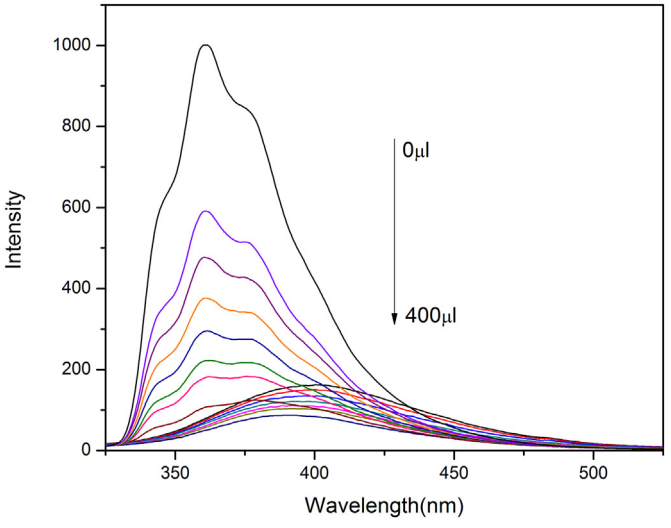

Fig. 13. Effect of NaOH adding on the emission spectra of **6c** (λ_{ex} = 287 nm).

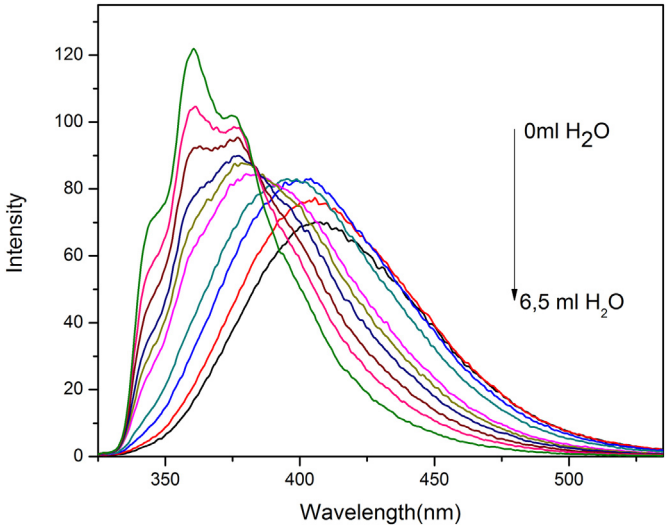

Fig. 14. Influence of the water content on the emission spectra of **6c** in DMSO solution (λ_{ex} = 287 nm).

Declaration of competing interest

The authors declare no competing financial interests or personal relationships that could have appeared to influence the work reported in this paper.

Appendix A. Supplementary data

Supplementary data to this article can be found online at https://doi.org/10.1016/j.molliq.2020.113196.

References

[1] E.S. Roesch, Isoquinolines, in: S. Brase (Ed.), Privileged Scaffolds in Medicinal Chemistry: Design, Synthesis, Evaluation, RSC, Cambridge 2015, pp. 147–213.
[2] D.A. Horton, G.T. Bourne, M.L. Smythe, The combinatorial synthesis of bicyclic privileged structures or privileged substructures, Chem. Rev. 103 (2003) 893–930.
[3] M. García-Castro, S. Zimmermann, M.G. Sankar, K. Kumar, Scaffold diversity synthesis and its application in probe and drug discovery, Angew. Chem. Int. Ed. 55 (2016) 7586–7605.
[4] P. Sau, S.K. Santra, A. Rakshit, B.K. Patel, *tert*-Butyl nitrite-mediated domino synthesis of isoxazolines and isoxazoles from terminal aryl alkenes and alkynes, J. Org. Chem. 82 (2017) 6358–6365.
[5] M.Y. Gang, J.Q. Liu, X.S. Wang, CuI-catalyzed Sonogashira reaction for the efficient synthesis of 1H-imidazo[2,1-a]isoquinoline derivatives, Tetrahedron 73 (2017) 4698–4705.
[6] R.G. Shi, J. Sun, C.G. Yan, Tandem double [3 + 2] cycloaddition reactions at both C-1 and C-3 atoms of N-cyanomethylisoquinolinium ylide, ACS Omega 2 (2017) 7820–7830.
[7] M. Leonardi, M. Villacampa, J.C. Menéndez, Mild and general synthesis of pyrrolo [2,1-a]isoquinolines and related polyheterocyclic frameworks from pyrrole precursors derived from a mechanochemical multicomponent reaction, J. Org. Chem. 82 (2017) 2570–2578.
[8] C.M. Al Matarneh, M.O. Apostu, I.I. Mangalagiu, R. Danac, Reactions of ethyl cyanoformate with cycloimmonium salts: a direct pathway to fused or substituted azaheterocycles, Tetrahedron 72 (2016) 4230–4238.
[9] L.W. Deady, T. Rodemann, G.J. Finlay, B.C. Baguley, W.A. Denny, Synthesis and cytotoxic activity of carboxamide derivatives of benzimidazo[2,1-a]isoquinoline and pyrido[3′,2′,4,5]imidazo[2,1-a]isoquinoline, Anticancer Drug Des. 15 (2000) 339–346.
[10] S.M. Rida, S.A.M. El-Hawash, H.T.Y. Fahmy, A.A. Hazzaa, M.M.M. El Meligy, Synthesis of novel benzofuran and related benzimidazole derivatives for evaluation of in vitro anti-HIV-1, anticancer and antimicrobial activities, Arch. Pharmacol. Res. 29 (2006) 826–833.
[11] R. Zhu, Y. Wang, J. Liu, Q. Wang, J. Huang, One-pot synthesis of imidazolyl isoquinolines under a palladium-catalyzed C-H activation/annulation (CHAA) reaction, Synthesis 49 (2017) 1335–1341.
[12] Y. Jiang, W. Kong, Y. Shen, B. Wang, Two fluorescence turn-on chemosensors based on pyrrolo[2,1-a]isoquinoline for detection of Ag^{+} in aqueous solution, Tetrahedron 71 (2015) 5584–5588.
[13] S.E. Kiruthika, A. Nandakumar, P.T. Perumal, Synthesis of pyrrolo-/indolo[1,2-a] quinolines and naphtho[2,1-b]thiophenes from gem-dibromovinyls and sulphonamides, Org. Lett. 16 (2014) 4424–4427.
[14] J. Krishnan, B. Vedhanarayanan, B.S. Sasidhar, S. Varughese, V. Nair, NHC-mediated synthesis of pyrrolo[2,1-a]isoquinolines and their photophysical investigations, Chem. Asian J. 12 (2017) 623–627.
[15] F. Zeng, Y. Jiang, B. Wang, C. Mao, Q. Han, Z. Ma, Self-organization of hyperbranched polyesters functionalized with pyrrolo[2,1-a]isoquinoline end groups and their fluorescent recognition of anthracene and pyrene, Macromol. Chem. Phys. 218 (2017), 1600616. .
[16] L. Leontie, I. Druta, R. Danac, M. Prelipceanu, G.I. Rusu, Electrical properties of some new high resistivity organic semiconductors in thin films, Prog. Org. Coat. 54 (2005) 175–181.
[17] S. Mahmoud, T. Aboul-Fadl, M. Sheha, H. Farag, A.M.I. Mouhamed, 1,2-Dihydroisoquinoline-N-acetic acid derivatives as new carriers for specific brain delivery I: synthesis and estimation of oxidation kinetics using multivariate calibration method, Arch. Pharm. Pharm. Med. Chem. 336 (2003) 573–584.
[18] J. Huckings, M.D. Johnson, N-substituted heterocyclic cations. IV. Rates and equilibria in the reactions of the N-cyano-quinolinium and -isoquinolinium ions in dilute aqueous acids. Some salt effects on the acidity function HR, J. Chem. Soc. (1964) 5371–5377.
[19] R. Chen, Y. Zhao, H. Sun, Y. Shao, Y. Xu, M. Ma, L. Ma, X. Wan, In situ generation of quinolinium ylides from diazo compounds: copper-catalyzed synthesis of indolizine, J. Org. Chem. 82 (2017) 9291–9304.
[20] L.R.R. Santin, S.C. dos Santos, D. La Rosa Novo, D. Bianchini, A.P. Gerola, G. Braga, W. Caetano, L.M. Moreira, E.L. Bastos, A.P. Romani, H.P.M. de Oliviera, Study between solvatochromism and steady-state and time-resolved fluorescence measurements of the methylene blue in binary mixtures, Dyes Pigments 119 (2015) 12–21.
[21] D. Maity, A. Mukherjee, S.K. Mandal, P. Roy, Modulation of fluorescence sensing properties of quinoline-based sensor for Zn^{2+}: application in cell imaging studies, J. Luminesc. 210 (2019) 508–518.
[22] X. Jia, X. Yu, X. Yang, J. Cui, X. Tang, W. Liu, W. Qin, A highly selective copper fluorescent indicator based on an aminoquinoline substituted BODIPY, Dyes Pigments 98 (2013) 195–200.
[23] N.K. Joshi, H.C. Joshi, R. Gahlant, N. Tewar, R. Ranteh, S. Tant, Steady state and time-resolved fluorescence study of isoquinoline: reinvestigation of excited state proton transfer, J. Phys. Chem. A 116 (2012) 7272–7278.